

Role of tRNA derived fragments in renal ischemia–reperfusion injury

Dan Li, Hao Zhang* , Xueqin Wu, Qing Dai, Shiqi Tang, Yan Liu, Shikun Yang and Wei Zhang*

Department of Nephrology, The Third Xiangya Hospital, Central South University, Changsha, China

ABSTRACT

Background: Ischemia–reperfusion injury (IRI) is one of the major causes of acute kidney injury (AKI). tRNA derived fragments (tRFs/tiRNAs) are groups of small noncoding RNAs derived from tRNAs. To date, the role of tRFs/tiRNAs in renal IRI has not been reported. Herein, we aimed to investigate the involvement of tRFs/tiRNAs in the occurrence and development of ischemia–reperfusion-induced AKI.

Methods: Moderate/severe renal IRI mouse models were established by bilateral renal pedicle clamping. The tRF/tiRNA profiles of healthy controls and moderate/severe IRI-stressed kidney tissues were sequenced by Illumina NextSeq 500. Candidate differentially expressed tiRNAs were further verified by RT-qPCR. Biological analysis was also performed.

Results: Overall, 152 tRFs/tiRNAs were differentially expressed in the moderate ischemic injury group compared with the normal control group ($FC > 2$, $p < 0.05$), of which 47 were upregulated and 105 were downregulated; in the severe ischemic injury group, 285 tRFs/tiRNAs were differentially expressed ($FC > 2$, $p < 0.05$), of which 157 were upregulated, and 128 were downregulated. RT-qPCR determination of eight abundantly expressed tiRNAs was consistent with the sequencing results. Gene Ontology analysis for target genes of the tRFs/tiRNAs showed that the most enriched cell components, molecular functions and biological processes were Golgi apparatus, cytoplasmic vesicles, protein binding, cellular protein localization and multicellular organism development. Kyoto Encyclopedia of Genes and Genomes (KEGG) analysis showed that these target genes were mainly involved in the natural killer cell mediated cytotoxicity pathway, citrate cycle, and regulation of actin cytoskeleton signaling pathway.

Conclusion: Our results indicated that tRFs/tiRNAs were involved in renal IRI. These tRFs/tiRNAs may be effective partly via regulation of renal immunity, inflammation and metabolism processes. Candidate genes, including tiRNA-Gly-GCC-003, tiRNA-Lys-CTT-003, and tiRNA-His-GTG-002, might be potential biomarkers and therapeutic targets of ischemia–reperfusion injury-induced acute kidney injury.

ARTICLE HISTORY

Received 26 October 2021

Revised 20 April 2022

Accepted 21 April 2022

KEYWORDS

tRNA derived fragments; ischemia–reperfusion injury; acute kidney injury

1. Introduction

Although some progress has been made in alternative treatment and management, the mortality rate of AKI patients receiving alternative treatment is still as high as 50% [1,2]. IRI is one of the main causes of AKI, which is caused by a transient decrease in renal blood flow and by restoration of the bloodstream and oxygen supply [3–5]. IRI is a dynamic process accompanied by inflammation, oxidative stress and lipid peroxidation [4], and it is mainly characterized by apoptosis of renal tubular cells and interstitial inflammation [6]. Although there is a certain understanding of the mechanism of IRI, little progress in the prevention or treatment of IRI-

induced AKI has been made thus far. Recent work has revealed that tRNA-derived small RNAs, also called tRNA derived fragments (tRFs/tiRNAs), are involved in kidney diseases [7,8]. tRFs/tiRNAs are a group of small noncoding RNAs derived from tRNAs and are mainly divided into two categories: tRNA-derived fragments (tRFs) and tRNA halves (tiRNAs, the following tRNA halves are abbreviated as tiRNAs in our present work). tRFs are derived from mature or precursor tRNAs with lengths of approximately 12–30 nucleotides. According to their position on tRNA, tRFs can be divided into five categories: tRF-5, tRF-3, tRF-1, 5′U-tRFs and i-tRFs. tRF-5 and tRF-3 are produced at the 5′ and 3′ ends of mature tRNA, respectively. 5′U-tRFs and tRF-1 are produced at

CONTACT Wei Zhang  weizhangxy@126.com  Department of Nephrology, The Third Xiangya Hospital of Central South University, No. 138, Tong zi po road, Changsha, 410013, Hunan Province, China

*Wei Zhang and Hao Zhang contribute equally to this work.

 Supplemental data for this article can be accessed [here](#).

© 2022 The Author(s). Published by Informa UK Limited, trading as Taylor & Francis Group.

This is an Open Access article distributed under the terms of the Creative Commons Attribution-NonCommercial License (<http://creativecommons.org/licenses/by-nc/4.0/>), which permits unrestricted non-commercial use, distribution, and reproduction in any medium, provided the original work is properly cited.

the 5' and 3' ends of the precursor tRNA. In addition, i-tRFs, as a new type of tRF, were discovered more recently. i-tRFs are completely inside the mature tRNA and can span anticodons [9].

tiRNAs are produced by the secreted ribonuclease angiogenin, which cleaves tRNA under stress conditions, such as oxidative stress and heat shock [10]. tiRNAs are divided into 5'-tRNA halves (5'-tiRNAs) with lengths of 30–35 nucleotides and 3'-tRNA halves (3'-tiRNAs) with lengths of 40–50 nucleotides [11]. Studies have shown that tRFs/tiRNAs are necessary for cells [12,13], as 5'-tRNAAla exerts a neuroprotective effect through the G-quadruplex structure [14], and tRF3E participates in the regulation of cancer cell growth by combining with nucleolin and increasing the expression of p53 [15]. Furthermore, tRFs/tiRNAs are also involved in the regulation of tumors [16], intergenerational inheritance of metabolic disorders [17], neurodegenerative diseases [14] and infections [12]. However, the role of tRFs/tiRNAs in IRI-induced AKI is not clear. Here, we performed comprehensive sequencing of tRFs/tiRNAs in renal tissues of an IRI-AKI mouse model. Through subsequent analysis and validation, we aimed to explore the possible relationship between tRNA derived fragments and renal IRI.

2. Materials and methods

2.1. Animals and experimental groups

Eighteen 8–9 weeks old C57BL/6 mice were obtained from Slyke jingda Biotechnology Company. All of them were fed under SPF-condition. Nine of them were randomly divided into three groups for tRFs/tiRNAs sequencing: Control group ($n=3$), moderate ischemic injury group (Ischemia 10 min and reperfusion 24 h, I10R, $n=3$), severe ischemic injury group (Ischemia 30 min and reperfusion 24 h, I30R, $n=3$). Later, another nine mice of the same age and background with the same grouping design were used for RT-qPCR verification.

2.2. Renal ischemia–reperfusion injury

After pentobarbital anesthesia, the bilateral renal pedicles of C57BL/6 mice were clamped for 10 or 30 min with microaneurysm clips (FST:18055-04) as previously reported [18]. After 10 min or 30 min of ischemia, the micro aneurysm clamps were released and blood flow of both kidneys recovered. After 24 h reperfusion, blood and renal tissues samples were taken and then stored in refrigerator at -80°C or fixed in 10% formalin for further processing.

2.3. Western blot

The expression of HIF-1 α in kidney tissues was detected by Western blot. Tissues were dissolved with RIPA buffer and PMSF and proteins extracted after mechanical homogenization. Then the supernatant lysate were forwarded to the total protein concentration measurement with the BCA protein assay kit (No.: P0012). The protein extract were incubated at 70°C for 10 min and separated by 8% SDS-polyacrylamide gel (protein amount was about $30\ \mu\text{g}/\text{lane}$). Then the gel was transferred to the polyvinylidene fluoride membrane. The membrane was blocked with 0.1% (w/v) BSA solution on a shaker for 2 h, then incubated with the HIF-1 α (Cat No.: 36169, Cell signaling technology) primary antibody at 4°C overnight, and finally incubated with the fluorescent secondary antibody for 1 h. The membranes were visualized by the Image Studio software and band intensities were quantified using Image J gel analysis software.

2.4. Measurement of serum creatinine and blood urea nitrogen

The blood of mice was collected 24 h after reperfusion and the supernatant were collected after centrifugation. Creatinine and urea nitrogen were measured on the biochemical analyzer in The Third Xiangya Hospital, Central South University.

2.5. Hematoxylin-eosin (H&E) staining and immunohistochemistry (IHC) of renal tissue

Fresh renal tissue was collected and immediately soaked in paraformaldehyde before embedding. The embedded kidney tissue was cut into $5\ \mu\text{m}$ for subsequent HE staining as previously described [19]. At least 10 high-power fields of view were randomly selected from each mouse and scored according to the area of tubular damage (0, no damage; 1, $<25\%$ damage; 2, $25\text{--}50\%$ damage; 3, $51\text{--}75\%$ damage; 4, $>75\%$ damage). Among them, renal tubular injury includes obvious expansion of renal tubule, disappearance of brush border, empty cannon of cell membrane and cytoplasm, cast, necrotic or exfoliated cells in the lumen, etc [20]. IHC was used to detect HIF-1 α and KIM-1 in tissues. Embedded tissue sections were dewaxed and then heated in a pressure cooker for 3 min to recover antigen. The washed sections were incubated in 3% H₂O₂ for 25 min at room temperature in the dark. Then, 3% BSA was added to the washed and dried sections for blocking at room temperature for 30 min. Next, the sections were incubated with the primary antibody

overnight at 4 °C. Antibody binding was detected using a peroxidase-conjugated secondary antibody for 30 min at 37 °C. DAB Substrate Kit for chromogenic reaction. Finally, dehydrate and mount.

2.6. tRFs/tiRNAs sequencing and data analysis

Renal cortex samples were collected and forwarded to tRFs/tiRNAs sequencing. The purity and concentration of total RNA samples were determined with NanoDrop ND-1000. Total RNA samples were pretreated to remove some RNA modifications that interfere with small RNA-seq library construction. Total RNA of each sample was sequentially ligated to 3' and 5' small RNA adapters. cDNA was then synthesized and amplified using Illumina's proprietary RT primers and amplification primers. Subsequently, 134–160 bp PCR amplified fragments were extracted and purified from the PAGE gel. And finally, the completed libraries were quantified by Agilent 2100 Bioanalyzer. The libraries were denatured and diluted to a loading volume of 1.3 mL and loading concentration of 1.8 pM. Diluted libraries were loaded onto reagent cartridge and forwarded to sequencing run on Illumina NextSeq 500 system using NextSeq 500/550 V2 kit (FC-404-2005, Illumina), according to the manufacturer's instructions. Raw sequencing data generated from Illumina NextSeq 500 that pass the Illumina chastity filter are used to the following analysis. Trimmed reads (trimmed 5', 3'-adaptor bases) are aligned allowing for 1mismatch only to the mature tRNA sequences, then reads that do not map are aligned allowing for 1mismatch only to precursor tRNA sequences with bowtie software. Based on alignment statistical analysis (mapping ratio, read length, fragment sequence bias), we determine whether the results can be used for subsequent data analysis. If so, the expression profiling and differentially expressed tRFs/tiRNAs are calculated. Principal component analysis (PCA), correlation analysis, pie plots, venn plots, hierarchical clustering, scatter plots and volcano plots are performed for the expressed tRFs/tiRNAs in R or Perl environment for statistical computing and graphics.

2.7. Gene ontology analysis and pathway analysis

The Gene Ontology (GO) project provides a controlled vocabulary to describe gene and gene product attributes in any organism (<http://www.geneontology.org>) [21]. The ontology covers three domains: Biological Process, Cellular Component and Molecular Function [22,23]. Fisher's exact test in Bioconductor's topGO is used to find if there is more overlap between the

differentially expression list and the GO annotation list than would be expected by chance. The p-value produced by topGO denotes the significance of GO terms enrichment in the differentially expressed genes. The lower the p-value, the more significant the GO Term (p-value <0.05 is recommended). KEGG analysis were conducted to analyze pathways involved in the target genes of our differentially expressed tiRNAs (<http://www.genome.jp/kegg/>) [24–26]. Pathway analysis is a functional analysis mapping genes to KEGG pathways. The p-value (EASE-score, Fisher-p-value or Hypergeometric-p-value) denotes the significance of the Pathway correlated to the conditions. Lower the p-value, more significant is the Pathway (The recommend p-value <0.05).

2.8. RNA extraction and reverse transcription PCR

Using Trizol reagent (Invitrogen life technologies) to isolate total RNA from renal cortex tissue samples according to the manufacturer's instructions. Before the sequencing experiment, use agarose gel electrophoresis and NanoDrop ND-1000 to check the concentration and purity of each RNA sample. Next, Using rtStar™ tRF&tiRNA Pretreatment Kit (Cat# AS-FS-005, Arraystar) to remove the modification of total RNA. Then, the RNA was reversed to cDNA. Next, polymerase chain reaction amplification was performed. The reaction mixture of the sample was first incubated in the StepOne real-time qPCR system for at 95 °C for 10 min, then 40 PCR cycles (95 °C for 10 s; 60 °C for 60 s). Table 1 lists the primer sequences used for RT-qPCR. U6 small nuclear RNA was used for normalization. The actual nucleotide sequence of the candidate tiRNAs is listed in Table 4.

Table 1. The primer sequence used in this study.

Gene	Primer sequence
U6	F:5'GCTTCGGCAGCACATATACTAAAAT3' R:5'CGCTTACGGAATTTGCGTGCAT3'
tiRNA-Gly-GCC-003	F:5'GCATTGGTGGTTCAGTGGTAG3' R:5'ACGTGTGCTCTCCGATCTC3'
tiRNA-Lys-CTT-003	F:5'ATCGCCCGGCTAGTCTAGT-3' R:5'GCTCTTCCGATCTGAGTCCCA3'
tiRNA-His-GTG-002	F:5'GATCGCCGTGATCGTATAGTG3' R:5'TTCCGATCTCAACGAGAGTA3'
tiRNA-Val-TAC-003	F:5'ACGATCGGTTCCATAGTGTAGC3' R:5'GCTCTTCCGATCTAAAGCAGAC-3'
tiRNA-Glu-TTC-002	F:5'AGTCCGACGATCTCCACAT3' R:5'GTGCTCTCCGATCTAAACCAG3'
tiRNA-Asp-GTC-002	F:5'GTCCGACGATCTCTCTGTTAG3' R:5'GTGCTCTTCCGATCTCAGGC3'
tiRNA-Ser-GCT-001	F:5'-CCGACGATCAAGAAAGATTGC-3' R:5'-TGTGCTCTCCGATCTCAGTTC-3'
tiRNA-Gly-CCC-004	F:5'-CCGCTGGTGTAGTGGTATCAT-3' R:5'-TGTGCTCTCCGATCTGAATC-3'

2.9. Statistical analysis

Data are expressed as mean \pm SD. Use two-tailed Student's *t*-test or nonparametric test for statistical comparison (SPSS 22.0). Statistical significance is defined as $p < 0.05$.

3. Results

3.1. Establishment of renal IRI models

The overall workflow of the present study is presented in Figure 1(A). By detecting serum creatinine, blood urea nitrogen and HE staining as well as HIF-1 α protein

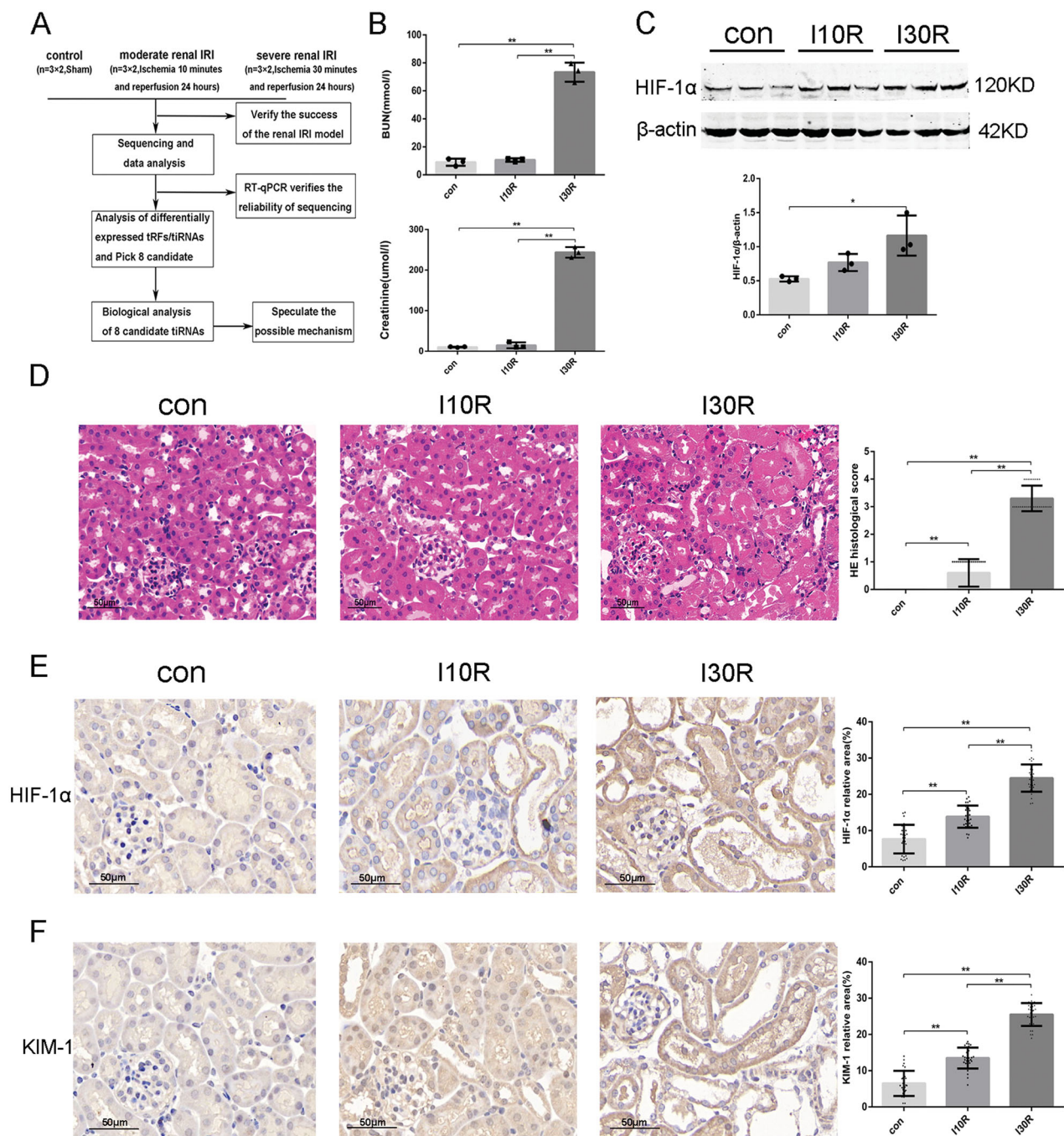


Figure 1. Establishment of renal IRI model. Blood urea nitrogen and serum creatinine levels (B) in control, moderate ischemic injury group (Ischemia 10 min and reperfusion 24 h, I10R, $n = 3$), severe ischemic injury group (Ischemia 30 min and reperfusion 24 h, I30R, $n = 3$). (C) Western blot analysis of HIF-1 α ($n = 3$). β -actin was used as loading control. All data were expressed as means \pm SD. * $p < 0.05$, ** $p < 0.01$. (D) HE staining of each group. Scale bar = 50 μ m. (E) Immunohistochemistry of HIF-1 α . (F) Immunohistochemistry of KIM-1.

expression in kidney tissue, we confirmed that the IRI models of both moderate and severe kidney injury were successfully established. As shown in Figure 1, compared with the control group, the creatinine and urea nitrogen levels in the I10R group did not change, but HE staining showed slight renal tubular damage. The creatinine and urea nitrogen levels in the I30R group were significantly increased, and the renal tubular damage was also more serious than in the control group and I10R group. IHC staining of the renal injury biomarker KIM-1 also confirmed the moderate injury of kidney tissue in the I10R group and overt injury in the I30R group. In addition, the expression of HIF-1 α in the I10R group was slightly increased, while it was remarkably upregulated in the I30R group compared to the control group. These data together confirmed that the moderate IRI renal injury and severe IRI renal injury models were successfully established.

3.2. Differential expression of tRFs/tiRNAs in IRI and control mice

Kidney tissues of mice with moderate and severe renal IRI were subjected to high-throughput sequencing to investigate the involvement of tRFs/tiRNAs in IRI-induced AKI. The quality score plot of each sample was plotted and is presented in Table 2. The Q score of each sample exceeded 30 (>99.9% correct), and BaseQ30 (%) exceeded 90%. In addition, the correlation coefficient analysis showed that the correlation coefficient in intra-group samples was significantly higher than that between the groups, which indicated that the reproducibility of the data was extremely high. In addition, principal component analysis (PCA) showed that the reproducibility of the samples within the group was high, and the differences in samples between the groups were clear. These data all confirmed the high quality of the samples.

Table 2. Quality score.

Sample	TotalRead	TotalBase	BaseQ30	BaseQ30 (%)
NC1	7981530	407058030	384083431	94.36
NC2	9040402	461060502	422753625	91.69
NC3	7720163	393728313	358652356	91.09
I10R1	6328573	322757223	293675187	90.99
I10R2	8142635	415274385	383169445	92.27
I10R3	8515670	434299170	400174645	92.14
I30R1	8639293	440603943	403825764	91.65
I30R2	8376463	427199613	392863566	91.96
I30R3	8975546	457752846	421228196	92.02

Sample: Sample name.

TotalRead: Raw sequencing reads after quality filtering.

TotalBase: Number of bases after quality filtering.

BaseQ30: Number of bases of Q score more than 30 after quality filtering.

BaseQ30 (%): The proportion of bases (Q \geq 30) number after quality filtering.

Overall, 687 tRFs/tiRNAs were detected by sequencing. The proportion of each subtype in each group is shown in Supplementary Figure 1(C–E). The number of tRF/tiRNA subtypes for tRNA isodecoders and the frequency of the subtypes for tRF/tiRNA length are presented in Supplementary Figure 2. In the I10R group, 152 tRFs/tiRNAs were differentially expressed (fold change >2 vs. control, $p < 0.05$), of which 47 were upregulated, and 105 were downregulated, and 285 tRFs/tiRNAs were differentially expressed in the I30R group, of which 157 were upregulated, and 128 were downregulated. There were 44 tRFs/tiRNAs that had increased expression in both the I10R group and the I30R group. Sixty-four tRFs/tiRNAs had decreased expression in both groups compared with the control group. A volcano plot (FC > 2, $p \leq 0.5$) shows the differential expression between the I10R, I30R and control groups (Figure 2(A,B)). Meanwhile, a heatmap showing the differentially expressed tRFs/tiRNAs is also presented with a heatmap summary (Figure 2(C,D)).

3.3. RT-qPCR verification of candidate tiRNAs

To verify the reliability of the high-throughput sequencing, eight tiRNAs that were relatively more abundant among the 16 tiRNAs out of 108 tRFs/tiRNAs (differentially expressed in both the I10R group and I30R group) were selected, and the expression of these tiRNAs was validated by RT-qPCR. The RT-qPCR results showed that the expression of tiRNA-Ser-GCT-001 was decreased in both ischemic groups, and the other seven tiRNAs (tiRNA-Asp-GTC-002, tiRNA-Glu-TTC-002, tiRNA-Gly-CCC-004, tiRNA-Gly-GCC-003, tiRNA-His-GTG-002, tiRNA-Lys-CTT-003 and tiRNA-Val-TAC-003) were all increased in I10R and I30R (Figure 3). These data were consistent with the sequencing results, thus confirming the reliability of the high-throughput sequencing.

3.4. Biological analysis of candidate tiRNAs

After verification by RT-qPCR, the eight candidate tiRNAs were forwarded for further bioinformatic analysis. GO analysis showed that the target genes of these tiRNAs are strongly involved in biological processes, including cellular protein localization, multicellular organism development, regulation of transcription, DNA-templated, peptidyl-tyrosine dephosphorylation, and citrate metabolic processes. These may also be associated with cell components, such as the Golgi apparatus, cytoplasmic vesicles, membrane, endoplasmic reticulum, and plasma membrane. These tiRNAs may also be effective in the regulation of molecular

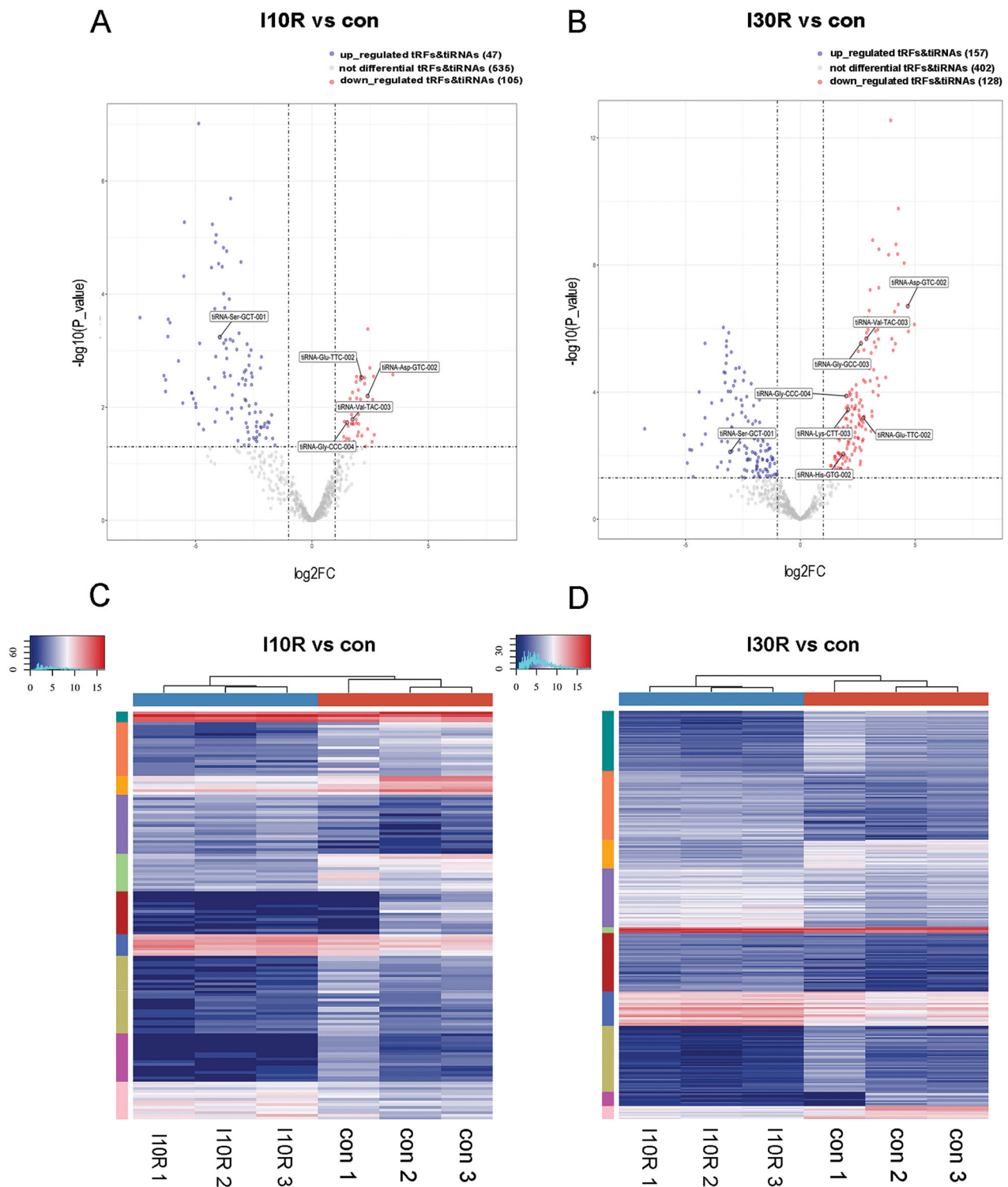


Figure 2. Differential expression of tRFs/tiRNAs in IRI and control mice. The volcano plot of tRFs/tiRNAs in I10R (A) and I30R (B). Purple/pink circles indicate statistically significant differentially expressed tRFs/tiRNAs with fold change >2 and p -value <0.05 (Purple: up-regulated; Pink: down-regulated). Gray circles indicate non-differentially expressed tRFs/tiRNAs, with FC and/or q -value are not meeting the cutoff thresholds. The hierarchical clustering heatmap for tRFs/tiRNAs. Blue represents an expression level below the mean, and red represents an expression level above the mean. (C) I10R vs con. (D) I30R vs con.

functions, including protein binding, epidermal growth factor receptor binding, metal ion binding, and sequence-specific DNA binding (Figure 4(A)).

KEGG analysis showed that the most relevant pathways possibly regulated by these tiRNAs in IRI conditions were natural killer cell-mediated cytotoxicity,

These pathways were all related to immunity, inflammation, energy metabolism and cell death.

Other target gene analysis of these candidate tiRNAs showed that the target genes of six tiRNAs were closely related to the regulation of cell death. Among the six tiRNAs, tiRNA-Lys-CTT-003 had the most target genes related to cell death, including *Unc5b*, *Bnip1*, *Zfp385a*, and *Ccr5*. tiRNA-Glu-TTC-002 also had many target genes associated with cell death, including *Naip6*, *Prf1*, *Sfrp4*, *Grid2*, and *Mindy3*. The target genes of tiRNA-His-GTG-002, such as *Mapk1*, *Scx*, *Ror1*, *Tchp* and *Erp29*, were also related to the regulation of cell death. tiRNA-Gly-GCC-003 also related to cell death, such as *Ntrk3* and *Ifi204*. These data suggested that dysregulated tiRNAs are strongly involved in several types of cell death, which are direct features of acute kidney injury.

4. Discussion

tRNA derived fragments are types of noncoding small RNAs, and their potential biological functions have gradually attracted increasing attention [27]. To date, studies have shown that tRFs/tiRNAs can regulate cell proliferation [28], differentiation [8], apoptosis and survival [29]. tRFs/tiRNAs are also related to some biological processes, such as gene silencing, regulatory translation and stress granule groups [30]. In the present study, we investigated the involvement of tRFs/tiRNAs in IRI-induced renal injury. To explore the initial and early changes in tRFs/tiRNAs in response to different degrees of ischemic injury, we established mouse models of kidney injury with moderate (10 min)/severe (30 min) ischemia and 24 h reperfusion. First, we found that a large number of tRFs/tiRNAs were enriched and differentially expressed in the IRI models compared with control mice. In moderate renal IRI mice, 152 tRFs/tiRNAs were differentially expressed, while 285 tRFs/tiRNAs were differentially expressed in severe renal IRI mice. Of note, only a small portion was consistently differentially expressed in both groups, which suggests that the gene expression profile of moderate ischemia or early ischemia is different from that of severe IRI injury of the kidney. Exploring earlier changes may help us find more and better biomarkers as well as therapeutic targets against IRI-induced AKI. We also found that there were 44 tRFs/tiRNAs that had increased expression in both the I10R group and I30R group. Sixty-four tRFs/tiRNAs had decreased expression in both groups compared with the control group. This part of the consistently changed tRFs/tiRNAs was helpful for us to explore the pathological mechanism of IRI.

To further explore the connections and potential mechanisms of tiRNAs and renal IRI, we selected eight candidates according to the sequencing results. GO analysis revealed that their predicted target genes were involved in many biological processes, including cellular protein localization, multicellular organism development, transcriptional regulation, and DNA templating. These may also be associated with cell composition, such as the Golgi apparatus and cytoplasmic vesicles. Additionally, these target genes were effective in the regulation of molecular functions, including protein binding and epidermal growth factor receptor binding. All of these biological processes, cellular components and molecular functions undoubtedly play essential roles in IRI-induced AKI [31,32]. Like PKC beta II, which was distributed in the cytoplasm of sloughed cells in the damaged PTEC, it was slightly expressed along the basal and lateral sides of the undamaged proximal tubular epithelial cells. The induced expression, translocation, and intracellular spatial distributions of the enzymes suggest that they may mediate multiple processes during IRI [31]. The increase in epidermal growth factor binding in the kidney after IRI injury and the attenuation of the increase in serum creatinine concentration by administration of exogenous epidermal growth factor suggest a role for epidermal growth factor in recovery from ischemic damage [33]. In addition, it has been reported that the absence of heparin binding-epidermal growth factor and inhibition of the EGF receptor in the early phase of IRI have protective effects, suggesting a modulating role of heparin binding-epidermal growth factor [34].

KEGG analysis showed that the predicted target genes of these tiRNAs were mainly enriched in signaling pathways related to immunity and inflammation, including natural killer cell-mediated cytotoxicity, the citrate cycle (TCA cycle), regulation of the actin cytoskeleton, the T-cell receptor signaling pathway, and the Toll-like receptor signaling pathway. Although little attention has been given to immune inflammation in renal IRI, some studies have shown that they play an important regulatory role in AKI caused by IRI [35]. *In vivo* experiments from Zhu-Xu Zhang et al. demonstrated that NK cells can directly kill TECs and that NK cells contribute substantially to kidney IRI [36]. Studies have shown that, after being activated by drugs, natural killer T cells can weaken the hypoxic injury of renal tubular epithelial cells through the hypoxia-inducible factor (HIF) and IL-10 pathways, thereby protecting the kidney from IRI [37]. On the contrary, it was also reported that cytokines, such as IL-33 and IL-12, can promote the recruitment of natural killer T cells,

Table 3. Target genes associate with cell death in tiRNAs.

tiRNAs	Target genes associate with cell death		
	Cell death	Regulation of cell death	Regulation/negative regulation of cell death
tiRNA-Asp-GTC-002	–	Ecdscr, Skp2	Ung, Shc1, Zpr1, Eya1, Ncam1
tiRNA-Glu-TTC-002	Dnase1l3, Prf1, Pnpla8, Mindy3	Prmt2, Sfrp4, Grid2	Naip6, Rhbdd1, Dnaja1, Fank1
tiRNA-Gly-CCC-004	–	–	Alk, Ncoa3, Pax2
tiRNA-Gly-GCC-003	lfi204	–	Ntrk3
tiRNA-His-GTG-002	Mapk1, Tchp	Erp29	Scx, Sox8, Ror1, Tldc1
tiRNA-Lys-CTT-003	Bnip1	Tctn3, Scrib	Mif, Unc5b, Zfp385a, Pou3f3, Dhcr24, Nfe2l2, Dusp6, Ccr5, Ppp5c

Table 4. The actual nucleotide sequence of the candidate tiRNAs.

tiRNAs	Actual nucleotide sequences
tiRNA-Asp-GTC-002	TCCTCGTTAGTATAGTGGTTAGTATCCCCGCTG
tiRNA-Glu-TTC-002	TCCCACATGGTCTAGCGGTTAGGATTCTGGTTT
tiRNA-Gly-GCC-003	GCATTGGTGGTTCAGTGGTAGAATTCTCGCCTG
tiRNA-Gly-CCC-004	GCCCGCTGGTGTAGTGGTATCATGCAAGATTC
tiRNA-Lys-CTT-003	GCCCGCTAGCTCAGTCGGTAGAGCATGGGACTC
tiRNA-Ser-GCT-001	AAGAAAGATTGCAAGAACTG
tiRNA-Val-TAC-003	GGTTCCATAGTGTAGCGGTTATCACGCTGCTTT
tiRNA-His-GTG-002	GCCGTGATCGTATAGTGGTTAGTACTCTGCGTTG

thereby exacerbating renal IRI [38]. Meanwhile, cell metabolism, mostly the citric acid cycle, was largely affected during renal IRI and was closely regulated by HIF [39]. In addition, the T cell receptor signaling pathway and Toll-like receptor signaling pathway were all involved in the processes of IRI-induced kidney injury [40–43]. On the other hand, the target genes of six tiRNAs of these eight candidates were also closely related to cell death regulation, as shown in Table 3.

Among these target genes, Rac1, Vav2, Mapk1 and Shc1 participate in multiple signaling pathways and are the target genes of tiRNA-Gly-GCC-003, tiRNA-Lys-CTT-003, tiRNA-His-GTG-002 and tiRNA-Asp-GTC-002. Previous studies have shown that these genes are closely related to IRI. Rac1 plays a key role in the process of renal fibrosis after ischemia–reperfusion injury by regulating the expression of profibrotic factors and chemokines, recruiting bone marrow-derived M2 macrophages, as well as transforming into myofibroblasts [44]. TRPM2 mediates ischemic kidney injury and oxidative stress through Rac1 [45]. It has been reported that Vav2-mediated activation of NADPH oxidase is an important mechanism for high homocysteine glomerular damage by enhancing local oxidative stress [46]. Studies have shown that inhibiting Ras/ERK1/2 (Mapk family) signaling can prevent ischemic kidney injury [47]. It has been proven that the mitochondrial-targeted antioxidant peptide SS31 has a protective effect on renal tubular epithelial cell apoptosis induced by ischemia–reperfusion by downregulating p66shc [48];

long-term exposure to nicotine can activate p66shc transcription to increase renal oxidative stress and damage [49]. All of these target gene bioinformatic analyses suggest a comprehensive and fundamental role for tiRNAs in the onset, progression as well as recovery of IRI-induced AKI. This will become a potential mechanism for our future research to optimize AKI prevention strategies.

Of course, our present work has many limitations since this was an initial sequencing profile with rough prediction and analysis without further detailed functional experimental verification. More extensive work on these tRFs/tiRNAs in the AKI context is needed in future research.

5. Conclusions

Our results indicate that tRFs/tiRNAs are involved in renal IRI. These tRFs/tiRNAs might be effective molecules partly by regulating renal immunity/inflammation, metabolism and cell death processes. Candidate tiRNAs, including tiRNA-Gly-GCC-003, tiRNA-Lys-CTT-003, and tiRNA-His-GTG-002, might be potential biomarkers and therapeutic targets in future research.

Author contribution statement

Wei Zhang and Hao Zhang designed this research study and revised the manuscript draft, Dan Li performed experiment, data analysis and manuscript composition; Xueqin Wu, Qing Dai, Yan Liu, Shiqi Tang and Shikun Yang contributed to the data analysis. All the authors read and approved the final version of the manuscript.

Disclosure statement

The authors declare that there is no conflict of interest regarding the publication of this paper.

Funding

The study was supported by grants from the National Natural Sciences Foundation of China [No. 81870498, No. 81900633], the Natural Sciences Foundation of Hunan Province [No. 2021JJ40954] and the Fundamental Research Funds for the Central Universities of Central South University [2019zzts909].

Ethics statement

This study (NO: 2019-S054) was approved by the IRB of Third Xiangya Hospital, Central South University. During the whole experiment, all experiments were performed in accordance with relevant guidelines and regulations by the IRB of Third Xiangya Hospital, Central South University.

Statement

The study is reported in accordance with ARRIVE guidelines.

ORCID

Hao Zhang  <http://orcid.org/0000-0002-2049-3485>

Data availability statement

The raw data of experiments used to support the findings of this study are available from the corresponding author upon request.

References

- [1] Koza Y. Acute kidney injury: current concepts and new insights. *J Inj Violence Res.* 2016;8(1):815–62.
- [2] Levey AS, James MT. Acute kidney injury. *Ann Intern Med.* 2017;167(9):ITC66–ITC80.
- [3] Hou J, Rao M, Zheng W, et al. Advances on cell autophagy and its potential regulatory factors in renal ischemia-reperfusion injury. *DNA Cell Biol.* 2019;38(9):895–904.
- [4] Malek M, Nematbakhsh M. Renal ischemia/reperfusion injury; from pathophysiology to treatment. *J Renal Inj Prev.* 2015;4(2):20–27.
- [5] Eltzhig HK, Eckle T. Ischemia and reperfusion—from mechanism to translation. *Nat Med.* 2011;17(11):1391–1401.
- [6] Loverre A, Ditunno P, Crovace A, et al. Ischemia-reperfusion induces glomerular and tubular activation of proinflammatory and antiapoptotic pathways: differential modulation by rapamycin. *J Am Soc Nephrol.* 2004;15(10):2675–2686.
- [7] Khurana R, Ranches G, Schafferer S, et al. Identification of urinary exosomal noncoding RNAs as novel biomarkers in chronic kidney disease. *RNA.* 2017;23(2):142–152.
- [8] Shi H, Yu M, Wu Y, et al. tRNA-derived fragments (tRFs) contribute to podocyte differentiation. *Biochem Biophys Res Commun.* 2020;521(1):1–8.
- [9] Aristeidis GT, Phillippe L, Shozo H, et al. Dissecting tRNA-derived fragment complexities using personalized transcriptomes reveals novel fragment classes and unexpected dependencies. *Oncotarget.* 2015;6(28):24797–822.
- [10] Yamasaki S, Ivanov P, Hu G-F, et al. Angiogenin cleaves tRNA and promotes stress-induced translational repression. *J Cell Biol.* 2009;185(1):35–42.
- [11] Anderson P, Ivanov P. tRNA fragments in human health and disease. *FEBS Lett.* 2014;588(23):4297–4304.
- [12] Wang Q, Lee I, Ren J, et al. Identification and functional characterization of tRNA-derived RNA fragments (tRFs) in respiratory syncytial virus infection. *Mol Ther.* 2013;21(2):368–379.
- [13] Soares AR, Fernandes N, Reverendo M, et al. Conserved and highly expressed tRNA derived fragments in zebrafish. *BMC Mol Biol.* 2015;16:22.
- [14] Ivanov P, O'Day E, Emara MM, et al. G-quadruplex structures contribute to the neuroprotective effects of angiogenin-induced tRNA fragments. *Proc Natl Acad Sci U S A.* 2014;111(51):18201–18206.
- [15] Falconi M, Giangrossi M, Zabaleta ME, et al. A novel 3'-tRNAGlu-derived fragment acts as a tumor suppressor in breast cancer by targeting nucleolin. *Faseb J.* 2019;33(12):13228–13240.
- [16] Sun C, Fu Z, Wang S, et al. Roles of tRNA-derived fragments in human cancers. *Cancer Lett.* 2018;414:16–25.
- [17] Chen Q, Yan M, Cao Z, et al. Sperm tsRNAs contribute to intergenerational inheritance of an acquired metabolic disorder. *Science.* 2016;351(6271):397–400.
- [18] Sung SJ, Li L, Huang L, et al. Proximal tubule CD73 is critical in renal ischemia-reperfusion injury protection. *J Am Soc Nephrol.* 2017;28(3):888–902. 1533-3450 (Electronic).
- [19] Hu Z, Zhang H, Yi B, et al. VDR activation attenuate cisplatin induced AKI by inhibiting ferroptosis. *Cell Death Dis.* 2020;11(1):73.
- [20] Xie Y, Liu B, Pan J, et al. MBD2 mediates septic AKI through activation of PKC η /p38MAPK and the ERK1/2 axis. *Mol Ther Nucleic Acids.* 2021;23:76–88.
- [21] The Gene Ontology Consortium. The gene ontology resource: 20 years and still going strong. *Nucleic Acids Res.* 2019;47(D1):D330–D338.
- [22] Li Z, Jiang C, Li X, et al. Circulating microRNA signature of steroid-induced osteonecrosis of the femoral head. *Cell Prolif.* 2018;51(1):e12418.
- [23] Wang C, Liu H, Yang M, et al. RNA-seq based transcriptome analysis of endothelial differentiation of bone marrow mesenchymal stem cells. *Eur J Vasc Endovasc Surg.* 2020;59(5):834–842.
- [24] Kanehisa M, Furumichi M, Sato Y, et al. KEGG: integrating viruses and cellular organisms. *Nucleic Acids Res.* 2021;49(D1):D545–D51.
- [25] Kanehisa M. Toward understanding the origin and evolution of cellular organisms. *Protein Sci.* 2019;28(11):1947–1951.
- [26] Goto MKS. KEGG: Kyoto encyclopedia of genes and genomes. *Nucleic Acids Res.* 2000;28(1):27–30.
- [27] Sobala A, Hutvagner G. Transfer RNA-derived fragments: origins, processing, and functions. *Wiley Interdiscip Rev RNA.* 2011;2(6):853–862.

- [28] Lee YS, Shibata Y, Malhotra A, et al. A novel class of small RNAs: tRNA-derived RNA fragments (tRFs). *Genes Dev.* 2009;23(22):2639–2649.
- [29] Balatti V, Nigita G, Veneziano D, et al. tsRNA signatures in cancer. *Proc Natl Acad Sci USA.* 2017;114(30):8071–8076.
- [30] Emara MM, Ivanov P, Hickman T, et al. Angiogenin-induced tRNA-derived stress-induced RNAs promote stress-induced stress granule assembly. *J Biol Chem.* 2010;285(14):10959–10968.
- [31] Padanilam BJ. Induction and subcellular localization of protein kinase C isozymes following renal ischemia. *Kidney Int.* 2001;59(5):1789–1797.
- [32] Yao M, Rogers NM, Csanyi G, et al. Thrombospondin-1 activation of signal-regulatory protein- α stimulates reactive oxygen species production and promotes renal ischemia reperfusion injury. *J Am Soc Nephrol.* 2014;25(6):1171–1186.
- [33] Norman J, Tsau YK, Bacay A, et al. Epidermal growth factor accelerates functional recovery from ischaemic acute tubular necrosis in the rat: role of the epidermal growth factor receptor. *Clin Sci (Lond).* 1990;78(5):445–450.
- [34] Mulder GM, Nijboer WN, Seelen MA, et al. Heparin binding epidermal growth factor in renal ischaemia/reperfusion injury. *J Pathol.* 2010;221(2):183–192.
- [35] Day YJ, Huang L, Ye H, et al. Renal ischemia-reperfusion injury and adenosine 2A receptor-mediated tissue protection: the role of CD4+ T cells and IFN- γ . *J Immunol.* 2006;176(5):3108–3114.
- [36] Zhang ZX, Wang S, Huang X, et al. NK cells induce apoptosis in tubular epithelial cells and contribute to renal ischemia-reperfusion injury. *J Immunol.* 2008;181(11):7489–7498.
- [37] Yang SH, Lee JP, Jang HR, et al. Sulfatide-reactive natural killer T cells abrogate ischemia-reperfusion injury. *J Am Soc Nephrol.* 2011;22(7):1305–1314.
- [38] Ferhat M, Robin A, Giraud S, et al. Endogenous IL-33 contributes to kidney ischemia-reperfusion injury as an alarmin. *J Am Soc Nephrol.* 2018;29(4):1272–1288.
- [39] Koivunen P, Hirsila M, Remes AM, et al. Inhibition of hypoxia-inducible factor (HIF) hydroxylases by citric acid cycle intermediates: possible links between cell metabolism and stabilization of HIF. *J Biol Chem.* 2007;282(7):4524–4532.
- [40] Savransky V, Molls RR, Burne-Taney M, et al. Role of the T-cell receptor in kidney ischemia-reperfusion injury. *Kidney Int.* 2006;69(2):233–238.
- [41] Liu LJ, Yu JJ, Xu XL. Kappa-opioid receptor agonist U50448H protects against renal ischemia-reperfusion injury in rats via activating the PI3K/AKT signaling pathway. *Acta Pharmacol Sin.* 2018;39(1):97–106.
- [42] Wu H, Chen G, Wyburn KR, et al. TLR4 activation mediates kidney ischemia/reperfusion injury. *J Clin Invest.* 2007;117(10):2847–2859.
- [43] Leemans JC, Stokman G, Claessen N, et al. Renal-associated TLR2 mediates ischemia/reperfusion injury in the kidney. *J Clin Invest.* 2005;115(10):2894–2903.
- [44] Liang H, Huang J, Huang Q, et al. Pharmacological inhibition of Rac1 exerts a protective role in ischemia/reperfusion-induced renal fibrosis. *Biochem Biophys Res Commun.* 2018;503(4):2517–2523.
- [45] Gao G, Wang WW, Raghu KT, et al. TRPM2 mediates ischemic kidney injury and oxidant stress through RAC1. *J Clin Invest.* 2014;124(11):4989–5001.
- [46] Yi F, Xia M, Li N, et al. Contribution of guanine nucleotide exchange factor Vav2 to hyperhomocysteinemic glomerulosclerosis in rats. *Hypertension.* 2009;53(1):90–96.
- [47] Kong T, Liu M, Ji B, et al. Role of the extracellular signal-regulated kinase 1/2 signaling pathway in ischemia-reperfusion injury. *Front Physiol.* 2019;10:1038.
- [48] Zhao W-Y, Han S, Zhang L, et al. Mitochondria-targeted antioxidant peptide SS31 prevents hypoxia/reoxygenation-induced apoptosis by down-regulating p66Shc in renal tubular epithelial cells. *Cell Physiol Biochem.* 2013;32(3):591–600.
- [49] Arany I, Clark J, Reed DK, et al. Chronic nicotine exposure augments renal oxidative stress and injury through transcriptional activation of p66shc. *Nephrol Dial Transplant.* 2013;28(6):1417–1425.